JOURNAL OF MATERIALS SCIENCE 25 (1990) 4143–4149

The dielectric properties of alumina substrates for microelectronic packaging

J. S. THORP, M. AKHTARUZZAMAN, D. EVANS*
*School of Engineering and Applied Science, and *Department of Physics, University of Durham, Durham, UK*

The dielectric characterization of alumina substrate materials used in high-performance microelectronic packaging is described. These materials included both pure and impure polycrystalline substrates and, as a reference standard, pure and chromium-doped single crystals of alumina. For each material the permittivity (ε') and dielectric loss (ε'') has been measured over a frequency range of 0.5 kHz to 10 MHz, at room temperature, and correlated with the structure and composition as determined by supplementary techniques. At room temperature the pure substrates show the frequency independence of both ε' and ε'', characteristic of pure single-crystal material. The permittivity ($\varepsilon' = 10.1$) agrees closely with the average of the anisotropic values for the single crystal but the dielectric loss is an order of magnitude higher than in the single crystal, giving $\tan\sigma \approx 1.5 \times 10^{-3}$. The impure substrates compared with the pure, show a small increase in ε' and a marked, frequency-dependent increase in dielectric loss. Measurements have also been made in both the high- and low-temperature ranges (i.e. 20 to 600° C and 77 to 293 K, respectively) in order to establish the variation of permittivity with temperature and frequency. At temperatures below 200° C the temperature coefficient of permittivity, $[(\varepsilon' - 1)(\varepsilon' + 2)]^{-1} (\partial\varepsilon'/\partial T)_P$, is about 9×10^{-6} K^{-1} for the pure materials but this increases rapidly with impurity addition.

1. Introduction

Many separate disciplines are involved in the design and manufacture of high-performance microelectronics packages and among these, the evaluation of materials features prominently. The general form of a simplified microelectronic package is shown in Fig. 1, which relates to silicon technology. The chip is mounted centrally on a dielectric substrate and metal conductor tracks are printed on the substrate surface to provide, via the lead frame, electrical connections to the device. The type of package used to house the chip affects the performance increasingly as silicon devices become larger and operate greater power ratings and higher operating frequencies. One of the major problems encountered, especially in large high-speed devices, is that of heat dissipation. As a consequence of this it is important to choose materials which have matched thermal coefficients of expansion (TCEs) so that the device does not become stressed either during the temperature cycling inherent in the processing routes of manufacture or as a result of temperature rises during operation. For silicon it is generally accepted that the TCE is about 3×10^{-6} °C^{-1} and this has led to the widespread use of alumina-based substrates which afford good TCE matching and are also compatible with conventional co-firing ceramic techniques. From the point of view of maximizing the allowable heat dissipation, alumina suffers from having a relatively low thermal conductivity (K = 21 W m^{-1} K^{-1}). Several other choices of substrate have been suggested, such as the use of the higher thermal conductivity aluminium nitride (K = 200 W m^{-1} K^{-1}) or the recently developed glass ceramic on metal systems [1], but these do not yet provide cheap, easily produced alternatives to alumina, and are not currently in widespread use in microelectronic packaging. Consequently there is still a strong interest in alumina, partly because it forms a reference against which newer alternative materials may be judged and partly because there is a continuing need to establish the detailed dependence of the dielectric parameters on microstructure and impurity content so that the techniques used in the fabrication and processing routes of substrate production may be optimized.

In the present work the dielectric properties of four groups of alumina-based materials over the frequency range 500 Hz to 10 MHz were determined at room temperature and the variation of permittivity with temperature was also examined at temperatures up to 600° C. The four groups of material were (1) pure single-crystal alumina, (2) single-crystal alumina doped at low level with chromium, (3) nominally pure sintered polycrystalline alumina, and (4) impure (black) sintered polycrystalline alumina; of these the first two were used to improve reference data on well-characterized materials, while the latter two represented typical substrate materials used for microelectronic packaging.

0022–2461/90 $03.00 + .12

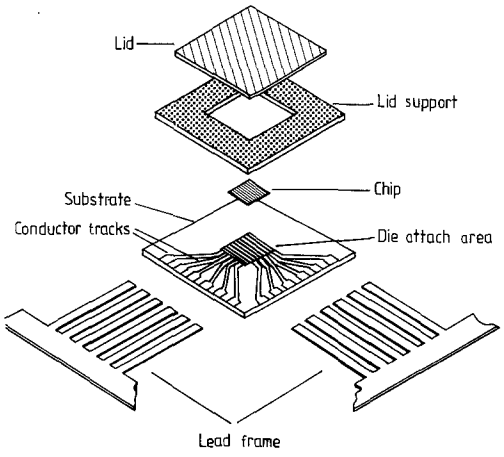

Figure 1 General features of a microelectronic package.

2. Experimental procedure

The permittivity (ε') and dielectric values were obtained from measurements made using bridge techniques and correction procedures similar to those used by Thorp and Rad [2] for dielectric examination of magnesium oxide and by Kenmuir *et al.* [3] for studying the dielectric properties of oxynitride glasses. From the materials available, disc-shaped specimens, usually of about 1.5 cm diameter and 0.05 cm thick, were cut out and the surfaces were polished using diamond paste to finishes of 0.25 μm. Circular gold electrodes were evaporated on to the polished faces to provide good electrical contact over a well-defined area of each disc. The width of the outer ring not covered by gold was chosen to reduce surface conduction over the edges of the disc to acceptable levels and appropriate edge corrections [4] were applied. For the high-temperature work, arrangements similar to those used by Thorp *et al.* [5] for studying the temperature dependence of permittivity in magnesium oxide were found to be suitable.

A variety of techniques was used to determine the chemical compositions, textures and microstructures of the specimens. These included X-ray diffraction (XRD). X-ray fluorescence (XRF), scanning electron microscopy (SEM), reflection high-energy electron diffraction (RHEED), and energy dispersive analysis by X-rays (EDAX) and are described in later sections where the characterization of each specimen is discussed.

3. Single-crystal alumina

3.1. Structural and analytical features

Aluminium oxide (Al_2O_3) has a trigonal unit cell with lattice parameters $a = 0.4758$ nm, $c = 1.2991$ nm [6]. For the growth of single-crystal alumina, both Czochralski and vapour-based methods of crystal growth [7] have been employed; both techniques can give a high degree of crystal perfection. In Czochralski growth, chromic oxide is used as the source of the chromium ions for doping alumina; single crystals containing other transition metal ions (e.g. titanium, iron, etc.) can be grown in a similar way. It is noticeable from the experimental evidence quoted in the literature (e.g. [8, 9]) that the crystal structure, orientation and degree of crystallinity, as well as the dopant or impurity, have a significant influence on the physical properties of the materials, and estimation of dopant concentration and of impurity content (either in the form of separate phases or replacement phases or replacement of the host ions) present in the system, is necessary to characterize the material. In the crystals used in the present investigations it was known from previous studies that both the crystal perfection and purity were exceedingly high; this was confirmed by RHEED examination, which revealed sharp diffraction spots and Kikuchi lines, and also by the clarity of the X-ray diffraction spots in back reflection X-ray photographs [10]. The pure alumina single crystal had an impurity content, as determined by mass spectrometry and XRF, of less than 10 p.p.m (chiefly iron) and the ruby contained 0.05% chromium. They thus formed useful reference standards against the effects of polycrystallinity or the deliberate introduction of additives could be assessed.

3.2. Room-temperature results

The crystals of pure and doped alumina were first examined at room temperature in the frequency range 0.5 to 30 kHz using a Wayne Kerr B 224 bridge and then by the Q-meter resonant technique which extended the frequency range to 10 MHz. The single-crystal samples were cut with their surfaces either parallel or perpendicular to the c-axis. The pure crystal results for the frequency variations of permittivity (ε') and dielectric loss (ε'') are shown in Fig. 2; here ε' is plotted in the form ($\varepsilon' - \varepsilon_\infty$) for reasons explained below.

These results are fairly close to the reported values of ε' [11–15] which are 9.3 (perpendicular to the c-axis) and 11.5 (parallel to the c-axis). The permittivities and dielectric losses for corresponding orientations of pure and doped crystals were the same.

One of the noticeable features of the behaviour of ε' and ε'' for the pure and chromium-doped single crystals is the frequency independence. The data have been fitted (see above) to the Universal Law of dielectric response [16] according to which the relations between the frequency and the permittivity, ε', or dielectric loss, ε'', can be expressed in the following form

$$(\varepsilon' - \varepsilon'_\infty) \propto \omega^{(n-1)} \tag{1}$$

and

$$\varepsilon'' \propto \omega^{(n-1)} \tag{2}$$

where ε'_∞ is the limiting value of the permittivity at high frequency, ω is the angular frequency and the exponent n is usually close to unity. For these pure and chromium-doped alumina single crystals the values of n are found to be 0.98 ± 0.02 from the ε' variation and $n = 0.96 \pm 0.04$ from the ε'' variation, where the value of ε'_∞ has been deduced from the optical refractive index ($\varepsilon'^{1/2}_\infty = 1.760$). The conductivity mechanism responsible for materials where the exponent approaches unity has been suggested by Jonscher to be screened hopping [17]. The addition of a very small percentage (0.05%) of chromium ion in the alumina lattice neither distorts the lattice significantly nor shows any appreciable change in the dielectric properties. Previous work on pure and doped single-crystal magnesium oxide [2], silicon nitride [18] and oxynitride glasses [3, 19]

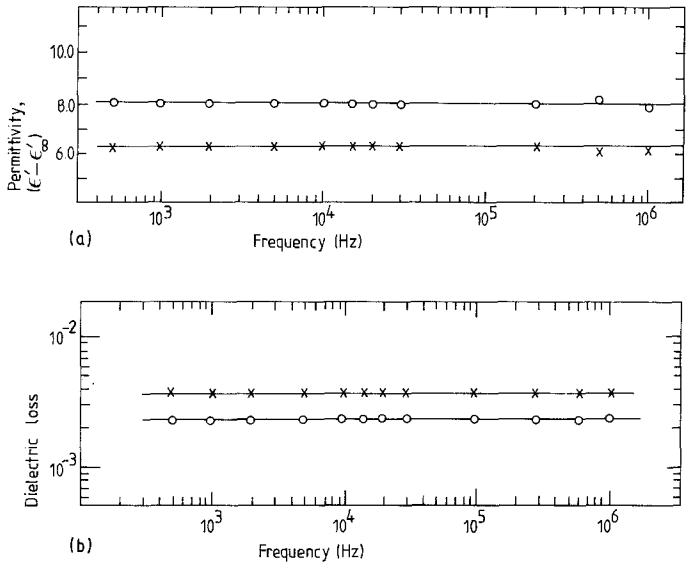

Figure 2 Frequency variations of (a) permittivity and (b) dielectric loss for Al_2O_3 single crystal. (x) Perpendicular to the c-axis, (○) parallel to the c-axis.

showed a similar type of behaviour. In these materials, the conduction mechanism was also believed to be hopping with n values very close to unity.

4. Pure polycrystalline alumina

4.1. Structural and analytical features

The polycrystalline alumina specimens examined were high-grade commercial substrates similar to those used for high-performance packaging. The available data (mainly from XRF) showed that the transition metal ion impurity levels were less than about 10 p.p.m. This material was made by well-established ceramic technologies, which involved high-temperature sintering of the green ceramic in oxygen ambients. Consequently, a fairly high-density product was obtained. Here the measured density was found to be 3.86 g cm^{-3} as compared with the X-ray density of 3.965 g cm^{-3}. This gives a packing fraction of 0.97. Several samples (of nominally the same composition, prepared by the same methods) were examined in the scanning electron microscope. This showed that the crystallite size was comparatively large – the mean size being about 5 μm – and that the boundaries appeared to be voids rather than containing a second crystalline phase. The same specimens were also examined by EDAX giving, as expected, a spectrum which revealed only an aluminum line, Fig. 3 (oxygen could not be detected by the instrument used). The lack of detectable signals by comparison with the signal intensities known to be obtained with given metal impurity levels, implied that the impurity concentrations were certainly less than 0.2%.

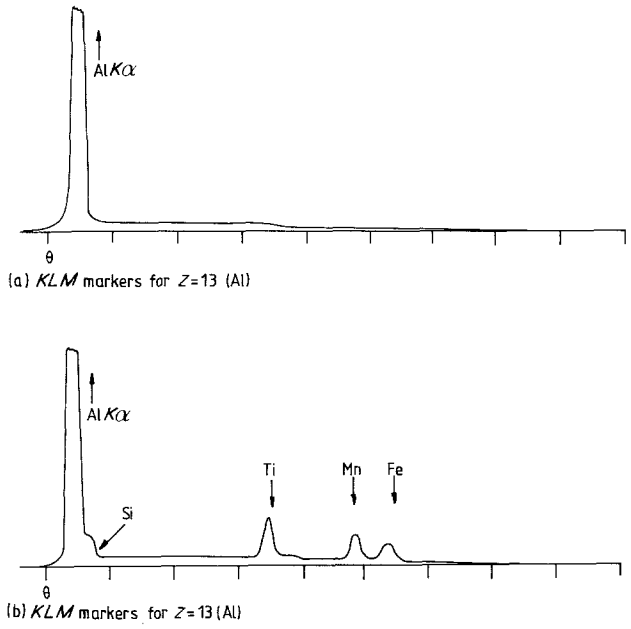

Figure 3 EDAX spectra for (a) pure polycrystalline alumina and (b) black polycrystalline substrates.

4.2. Room-temperature results

Measurememts were made over the same frequency range as was used for the single-crystal specimens. A correction was made for the measured porosity, and, on the assumption that the material contained only aluminium oxide grains and voids (air), the values of the equivalent solid permittivity and loss were determined. Thus, the experimentally measured permittivity (ε'_p) was converted to the equivalent solid value (ε'_s) by the relation

$$(\varepsilon'_p)^{1/3} - 1 = p[(\varepsilon'_s)^{1/3} - 1] \quad (3)$$

and the corresponding loss (ε''_p) to the equivalent solid loss (ε''_s) by

$$\varepsilon''_s = \frac{\varepsilon''_p}{p}\left[\frac{\varepsilon'_s}{\varepsilon'_p}\right]^{2/3} \quad (4)$$

where p is the packing fraction [20]. The experimental results are given in Fig. 4; it can be seen that again frequency-independent behaviour is observed both for the ε'_s and the ε''_s variations. The n values derived from the permittivity and loss data, again taking $\varepsilon'^{1/2}_\infty = 1.76$, were $n = 0.98 \pm 0.2$ and $n = 0.96 \pm 0.4$, respectively, which are in good agreement with each other. The magnitude of the permittivity, $\varepsilon'_s = 10.18$, is between the two limits of 11.4 and 9.4 for the parallel and perpendicular orientations of the single-crystal material, respectively. Assuming a completely random orientation of grains in the sintered material, the permittivity should be the arithmetic means of the two extreme values of the single-crystal, i.e. 10.4. The measured value is in good agreement with this, suggesting that there is very little, if

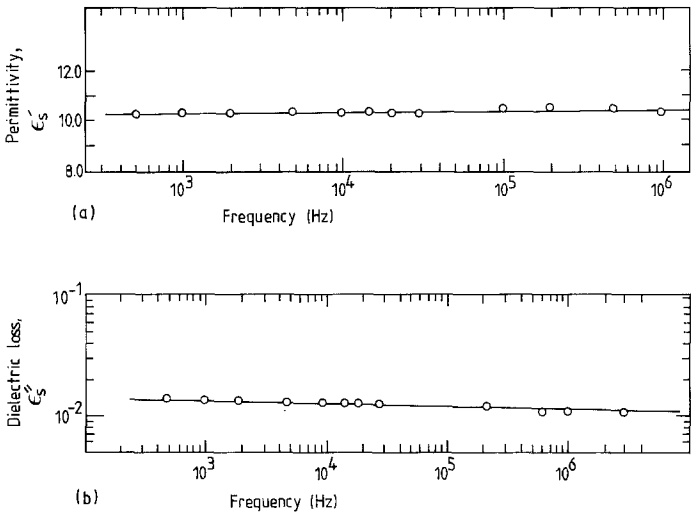

Figure 4 Frequency variations of (a) permittivity and (b) dielectric loss for pure polycrystalline alumina substrate.

any, preferred orientation in the specimen. This result was confirmed by black reflection X-ray examination, which shows continuous Debye–Sherrer rings with no evidence of arc formation.

The measured value of dielectric loss at 1 kHz of 1.4×10^{-2} is increased to give ε_s'' of 1.5×10^{-2} by allowing for the air in the voids. Comparison of ε_s'' for this pure polycrystalline alumina with the value of $\varepsilon'' = 3.0 \times 10^{-3}$ for the pure single-crystal material at the same frequency shows that the former is a factor five larger than the latter. The major difference between the two specimens is the presence of the grain boundaries. The SEM evidence, Fig. 5a, suggests a mean grain size of about 5 μm and so taking the dimensions of the sample used and assuming spherical particles, an estimate of the number of grain-boundaries can be made. Here the disc-shaped sample between the electrodes had a diameter of 6 mm and a thickness of 0.6 mm. With a 5 μm grain size there will be 1.2×10^3 grains across a diameter and 1×10^2 grains along the thickness. Hence in the total volume considered there will be approximately 1.1×10^8 grains, each of which is assumed to contribute one grain boundary. This shows that the introduction of 10^8 boundaries increases ε'' from 3×10^{-3} to 1.5×10^{-2} (i.e. tan δ from 3×10^{-4} to 1.4×10^{-2}); in the substrate context, either value is acceptable, but the comparison illustrates the degree of control which could be achieved by alteration of grain size if this were a viable option from manufacturing considerations.

5. Black alumina

5.1. Structural and analytical features

In some types of package there is a requirement for an optically opaque substrate in order to make the semiconductor circuits less susceptible to adverse effects caused by optical irradiation. By the addition of certain metal oxides (chiefly those of iron and manganese) the substrate can be made non-transparent and exhibits a black colouration; these materials are commonly termed "black alumina". Because the impedance of the input conductor leads to the chip are, in part, determined by the permittivity and loss of the substrate, it is of interest to ascertain what degree of opaqueness can be achieved without causing too large a rise in tan δ. Ideally tan δ values in the range 10^{-4} to 10^{-3} are preferred, but package designs could be made to accommodate tan δ values lying between 10^{-3} and 10^{-2} as an upper limit.

The samples of black alumina examined were chosen as representative of this type of commercially available ceramic and the main interest was to establish the effect of the relatively large concentration of additive on the dielectric properties. They were examined by several analytical techniques. X-ray fluorescent analysis showed that iron, manganese and titanium were present at levels of 1.5%, 1.5% and 1.1% respectively together with other metals (i.e. barium, zirconium, strontium, rubidium, zinc, copper, nickel, vanadium, chromium, and gallium) at trace levels not exceeding 100 p.p.m. This was confirmed by the EDAX spectra, e.g. Fig. 2b taken from a selection of

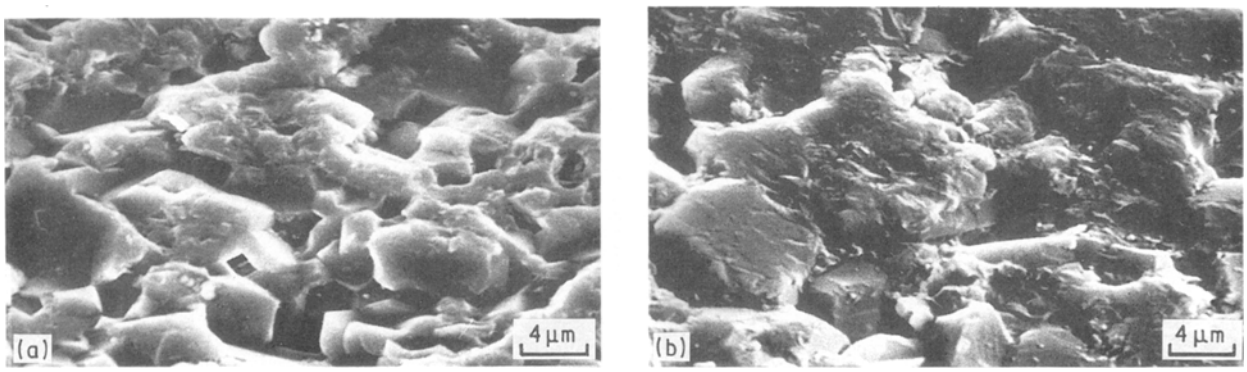

Figure 5 Scanning electron micrographs of (a) pure and (b) black alumina substrate material.

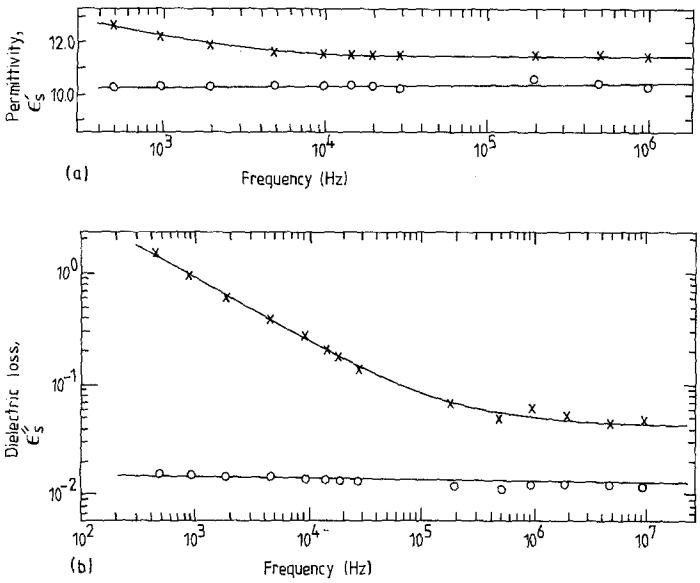

Figure 6 Frequency variations of (a) permittivity and (b) dielectric loss of (x) black polycrystalline alumina substrate material, compared with (○) pure polycrystalline alumina substrate.

areas of the sample, all of which showed clear peaks corresponding to iron, manganese and titanium. The scanning electron micrographs (e.g. Fig, 5b) show a relatively large grain size, ~ 10 μm on average, together with evidence for additional phases, of much smaller size, there appears to be segregation of the impurities to the grain boundaries.

5.2. Room-temperature results

As with other alumina samples, the black alumina specimens were examined over the frequency range 0.5 kHz to 10 MHz. The permittivity–frequency plot is shown in Fig. 6a, which includes for comparison the data for the pure polycrystalline alumina. Two features are evident. In the first place, there is some frequency dependence with ε'_s rising at low frequencies; above 10 kHz the values of ε' for black alumina are nearly the same as those for pure polycrystalline alumina, but at 0.5 kHz ε' is about 10% higher than ε' for pure alumina. The second feature relates to the corresponding data for the dielectric loss given in Fig. 6b. Here it is seen also that the loss is no longer frequency independent, rising markedly at the lower frequencies, and is also much greater than for the pure polycrystalline materials at all frequencies. This additional increase above the values for pure polycrystalline alumina must be attributed to the impurity additives The value of tan δ for the black alumina was 1.3×10^{-1} compared with 1.4×10^{-3} for the pure alumina at 0.5 kHz and 6×10^{-3} compared with 1.3×10^{-3} at 1 MHz. It is evident that the behaviour cannot be accounted for on the basis of the universal law of dielectric response. There is strong evidence that the overall dielectric properties of the black alumina are determined in a complex manner, not only by the space charge polarization at the grain boundaries but also by the dielectric and magnetic properties of the individual additives. The present result is very similar to that of Rao and Smakula [21], who attributed this effect to the space charge formation which depends on both the purity and perfection of the material; it has also been pointed out that the effect is noticeable mainly in the low-frequency region [22, 23].

6. Temperature coefficient of permittivity

The temperature variations of permittivity for the three types of alumina also were examined in the temperature range 20 to 700° C over the frequency range 0.5 to 20 kHz. The data for the reference single-crystal Cr/Al_2O_3 are shown in Fig. 7 together with the corresponding plots for the pure and impure polycrystalline alumina. For the single crystal, the permittivity–temperature plots show, at each frequency, that two distinctly dissimilar regions prevail, namely a linear region and an exponential region. The linear region for single-crystal material at 1.0 kHz extends up to about 270° C. It is important to note that the non-linearity commences at a lower temperature for the

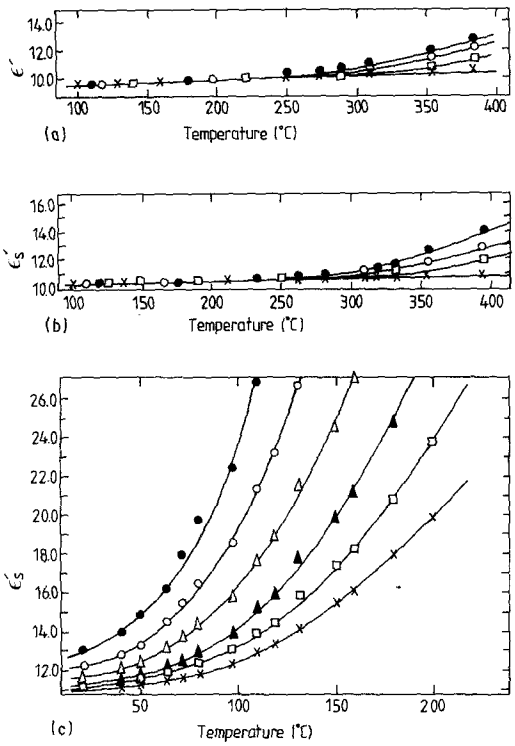

Figure 7 Temperature variation of permittivity for (a) single crystal alumina, (b) pure polycrystalline alumina and (c) black polycrystalline alumina; high-temperature range. Frequency (kHz): (●) 500, (○) 1, (△) 2, (▲) 5, (□) 10, (x) 20.

TABLE I Temperature coefficient for various aluminas compared with those of other oxide ceramics

Material	Temperature range (°C)	Temperature coefficient $[(\varepsilon' - 1)(\varepsilon' + 2)]^{-1} (\partial\varepsilon'/\partial T)_P$ (K^{-1})	Reference
Al_2O_3 single crystal (perp.)	105–540	8.3×10^{-6}	Present work
Pure Al_2O_3 polycrystalline substrate	85–540	9.2×10^{-6}	Present work
Black Al_2O_3 Polycrystalline substrate	105–180 180–293 293–320	11×10^{-6} 1.2×10^{-4} $> 5 \times 10^{-4}$	Present work
Sapphire single crystal (perp.)	5.5–380	8.9×10^{-6}	[25]
Sapphire single crystal (parallel)	5.5–380	1.1×10^{-5}	[25]
Quartz single crystal (parallel)	5.5–380	2.2×10^{-6}	[25]
Magnesia single crystal (parallel)	273–480	1.0×10^{-5}	[5]
Magnesia single crystal (parallel)	273–480	1.0×10^{-5}	[5]

lower frequencies and at relatively higher temperature for the higher frequencies. Comparison of the data for the three types of alumina examined in the present investigation shows that the extent of the linear region decreases with increasing crystalline imperfection (polycrystallinity) and almost disappear with the introduction of noticeable amounts of impurity. Similar high-temperature behaviour has been recently reported in magnesium oxide by Thorp *et al.* [5] and analysed in terms of temperature-enhanced conductivity.

Over the linear regions, the temperature coefficient of permittivity at constant pressure, P, $[(\varepsilon' - 1)(\varepsilon' + 2)]^{-1} (\partial\varepsilon'/\partial T)P$ for all the alumina samples were calculated, [24]. The data are given in Table I which also includes values for other oxide ceramic materials. The temperature coefficient of permittivity for the chromium-doped single-crystal alumina was $7.5 \times 10^{-6} K^{-1}$ which is quite comparable to the values for sapphire reported for single crystals studied at low temperatures [25]. For the pure polycrystalline alumina sample the coefficient slightly increases to $9.3 \times 10^{-6} K^{-1}$. It was impossible to calculate the temperature coefficient of permittivity for the impure black polycrystalline alumina on the same basis as the non-linearity started at room temperature. However, it is clear from the shape of the variation that the values of the coefficient, even if taken over limited temperature ranges, will be very large and will also increase rapidly as the temperature is raised.

Measurements were also made in the low-temperature range from 90 to 293 K. The results are shown in Fig. 8. For the single-crystal and pure polycrystalline alumina, the ε'–T plots are linear and there is no measurable frequency dispersion between 1 and 20 kHz; the values of the temperature coefficients are in close agreement with those obtained in the 20 to 270° C range. The black alumina behaves in a different way. On cooling below room temperature, the permittivity at first still changes quite rapidly (Fig. 8c), and there is also a residual frequency dependence of the same type as at higher temperatures. At temperatures below about 200 K these effects are no longer noticeable and, although the permittivity varies slightly with temperature, this variation is approximately linear. The Bosman and Havinga formula has been applied over limited temperature ranges in order to assess how the coefficient varies with temperature. It can be seen that in lowest temperature range (i.e. 100 to 180 K) the value is about $11.0 \times 10^{-6} K^{-1}$ which is

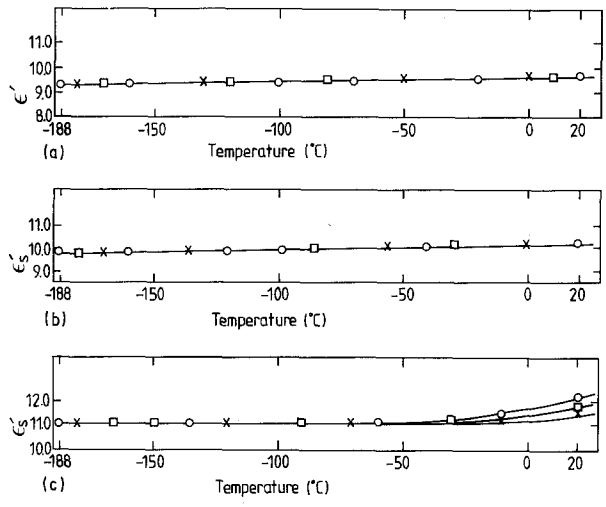

Figure 8 Temperature variation of permittivity for (a) single-crystal alumina, (b) pure polycrystalline alumina and (c) black polycrystalline alumina; low-temperature range. Frequency (kHz): (○) 1, (□) 10, (×) 20.

comparable to the values of $9.1 \times 10^{-6} K^{-1}$ and $9.15 \times 10^{-6} K^{-1}$ obtained for Cr/Al_2O_3 and pure polycrystalline alumina, respectively. At higher temperatures the coefficient increases rapidly, being $\sim 5 \times 10^{-4}$ in the range 20 to 50° C and at higher temperatures becomes strongly frequency dependent. Thus it appears that at sufficiently low temperatures the contribution from impurities (and presumably also from imperfection) is negligible. It is generally accepted that at low temperatures the imperfections [21] and impurities [23] present in a dielectric material do not have any influences on the dielectric properties, and the present data on impure alumina supports this view. At and above room temperature the coefficient is not only large but also frequency dependent. Thus, at an operating temperature of 50° C, the effective shunt capacity of the substrate to the input leads of the chip increases by 40% as the frequency changes from 20 to 0.5 kHz; at 85° C the shunt capacity doubles over the same frequency range. Recalling also that the value of tan δ is large and frequency dependent (Section 5.2. and Fig. 6b), one concludes that the stability of black alumina of the type investigated here, for high-quality packaging must be seriously questioned.

7. Conclusions

Dielectric data for the permittivity, dielectric loss and temperature coefficient of permittivity have been determined for substrate-grade specimens of pure crystalline alumina and for black polycrystalline alumina and compared with reference standards of single-crystal material. This has enabled the effects of polycrystallinity and of impurity content to be separately examined. It was found that for the pure polycrystalline alumina substrate the values of permittivity, tan δ and temperature coefficient of permittivity closely approached the single-crystal values, indicating a high-quality substrate material. The addition of impurities to give opaque (black) substrates is in general deleterious from the dielectric point of view and such an approach needs to be controlled with caution if the overall electrical specifications of the package are to be maintained.

Acknowledgements

We thank the SERC/Alvey High Performance Packaging Consortium through which some of the materials examined were obtained. One of us (M.A.) also thanks the University of Rajshahi, Bangladesh for the award of a Research Scholarship.

References

1. E. A. LOGAN, D. HOLLAND, J. S. THORP and G. PARTRIDGE, in Proceedings of the IEEE European Manufacturing Technology Symposium, Vol. 14 Paris, France (1988).
2. J. S. THORP and N. E. RAD, *J. Mater. Sci.* **16** (1981) 255.
3. S. V. J. KENMUIR, J. S. THORP and B. L. J. KULESZA, *ibid.* **18** (1983) 1725.
4. A. H. SCOTT and H. L. CURTIS, *J. Res. Nat. Bur. Stand.* **22** (1939) 747.
5. J. S. THORP, N. E. RAD, D. EVANS and C. D. H. WILLIAMS, *J. Mater. Sci.* **21** (1986) 3091.
6. W. LOW, *Phys. Rev.* **105** (1957) 801.
7. J. S. THORP, "Masers and Lasers: Physics and Design" (Macmillan, London, 1967).
8. A. K. CHAUDRY and K. V. RAO, *Phys. Status Solidi* **32** (1969) 731.
9. K. LAL and K. H. JHANS, *J. Phys. C.* **10** (1977) 1315.
10. M. AKHTARUZZAMAN, PhD thesis, University of Durham (1989).
11. J. FONTANELLA, C. ANDEEN and D. SCHUELE, *J. Appl. Phys.* **45** (1974) 2852.
12. S. GOVINDA and K. V. RAO, *Phys. Status Solidi (a)* **27** (1975) 639.
13. E. V. LOEWENSTEIN, D. R. SMITH and R. L. MORGAN, *Appl. Opt.* **12** (1973) 398.
14. E. E. RUSSELL and E. R. BELL *J. Opt. Soc. Amer.* **57** (1967) 341.
15. S. ROBERTS and D. D. COON, *ibid.* **52** (1962) 1923.
16. A. K. JONSHER, *Nature* **267** (1977) 673.
17. *Idem, ibid.*, **253** (1975) 717.
18. J. S. THORP, A. B. AHMAD, B. L. K. KULESZA and T. G. BUSHELL, *J. Mater. Sci.* **19** (1984) 3680.
19. J. S. THORP, S. V. J. KENMUIR, D. EVANS and N. E. RAD, *ibid.*, **23** (1988) 707.
20. H. LOOYENGA, *Physica* **31** (1965) 401.
21. K. V. RAO and A. SMAKULA, *J. Appl. Phys.* **36** (1965) 2031.
22. F. L. WEICHMAN, *Can. J. Phys.* **51** (1973) 680.
23. R. S. BEVER and R. L. SPROULL, *Phys. Rev.* **83** (1951) 801.
24. A. J. BOSMAN and E. E. HAVINGA, *Phys. Rev.* **129** (1963) 1593.
25. J. LINK, M. C. WINTERSGILL, J. J. FONTELLA, V. E. BEAN and C. G. ANDEEN, *J. Appl. Phys.* **52** (1981) 986.

Received 1 June
and accepted 6 October 1989